Received: 11 January 2022 | Revised: 14 May 2022 | Accepted: 18 May 2022

DOI: 10.1111/cas.15438

Cancer Science WILEY

ORIGINAL ARTICLE

Extracellular vesicles expressing CEACAM proteins in the urine of bladder cancer patients

Ko Igami[1,2,3] | Takeshi Uchiumi[3,4] | Masaki Shiota[5] | Saori Ueda[3] | Shigehiro Tsukahara[3,5] | Masaru Akimoto[3] | Masatoshi Eto[5] | Dongchon Kang[3]

[1]Business Management Division, Clinical Laboratory Business Segment, LSI Medience Corporation, Tokyo, Japan

[2]Kyushu Pro Search Limited Liability Partnership, Fukuoka, Japan

[3]Department of Clinical Chemistry and Laboratory Medicine, Kyushu University, Fukuoka, Japan

[4]Department of Health Sciences, Graduate School of Medical Sciences, Kyushu University, Fukuoka, Japan

[5]Department of Urology, Graduate School of Medical Sciences, Kyushu University, Fukuoka, Japan

Correspondence
Takeshi Uchiumi, Department of Clinical Chemistry and Laboratory Medicine, Graduate School of Medical Sciences, Kyushu University, 3-1-1 Maidashi, Higashi-ku, Fukuoka 812-8582, Japan.
Email: uchiumi@cclm.med.kyushu-u.ac.jp

Funding information
LSI Medience; Japan Society for the Promotion of Science (JSPS), Grant/Award Number: 17H01550, 18K15421, 20H00530; Japan Agency for Medical Research and Development (AMED), Grant/Award Number: JP21lm0203009.

Abstract

Early detection and long-term monitoring are important for urothelial carcinoma of the bladder (UCB). Urine cytology and existing markers have insufficient diagnostic performance. Here, we examined medium-sized extracellular vesicles (EVs) in urine to identify specific markers for UCB and evaluated their usefulness as diagnostic material. To identify specific markers in urinary EVs derived from UCB, we undertook shotgun proteomics using urine from four UCB patients and four healthy subjects. Next, 29 healthy specimens, 18 noncancer specimens, and 33 UCB specimens, all from men, were analyzed for urinary EVs by flow cytometry to evaluate the diagnostic performance of UCB-specific EVs. Nanoparticle-tracking analysis indicated that the size of EVs extracted from urine was mostly <400 nm. By shotgun proteomics, we detected several proteins characteristic of UCB and found that carcinoembryonic antigen-related adhesion molecule (CEACAM) proteins were increased in patients. Flow cytometric analysis revealed that the degree of expression of CEACAM1, CEACAM5, and CEACAM6 proteins on the surface of EVs varied among patients. Extracellular vesicles expressing CEACAM proteins also expressed mucin 1, suggesting that they were derived from tumorigenic uroepithelial cells. The number of EVs expressing CEACAM1, 5, and 6 proteins was significantly increased in UCB (mean ± SD, 8.6 ± 13%) compared to non-UCB (0.69 ± 0.46) and healthy (0.46 ± 0.34) by flow cytometry. The results of receiver operating characteristic (ROC) analysis showed a good score of area under the ROC curve of 0.907. We identified EVs that specifically express CEACAM proteins in urine and have potential for diagnostic applications. These EVs are potential targets in a new liquid biopsy test for UCB patients.

KEYWORDS
bladder cancer, CEACAM, extracellular vesicle, flow cytometry, proteomics

Abbreviations: CEACAM, carcinoembryonic antigen-related adhesion molecule; EV, extracellular vesicle; LFQ, label-free quantification; MUC1, mucin 1; NTA, nanoparticle-tracking analysis; OPLS-DA, orthogonal partial least squares discriminant analysis; ROC, receiver operating characteristic; THP, Tamm–Horsfall protein; UCB, urothelial carcinoma of the bladder.

1 | INTRODUCTION

Urothelial carcinoma of the bladder, the fourth most common cancer in men, results in significant morbidity and mortality.[1] It is ranked 6th or 7th in estimated cancer incidence in the United States to 2040.[2] At the time of initial diagnosis, approximately 70% of patients have cancer confined to the epithelium or subepithelial connective tissue. These cancers are usually treated with endoscopic resection and selective intravesical therapy. The recurrence rate of superficial disease exceeds 60%, and <30% of recurrent bladder tumors progress to invasive disease.[3] Thus, UCB requires continuous cystoscopy and cytology because of the high recurrence rate of the disease.[4,5] These tests are invasive and expensive, and there are differences among users and among the facilities that carry them out.

Urine-based biomarkers for the detection of UCB seem to be an attractive option. However, the FDA-approved test will not replace the current diagnostic criteria of urine cytology and cystoscopy, and more sensitive and specific biomarkers are needed.[6] There have been several reports of possible protein UCB markers in urine, including CEACAM1. Tilki et al. reported that urinary CEACAM1 levels discriminate between UCB patients and non-UCB subjects. Furthermore, urinary CEACAM1 levels increase with advancing stage and grade.[7]

Extracellular vesicles play essential roles in cell–cell communication and are diagnostically significant materials.[8–11] Extracellular vesicles are membrane vesicles that most cells release into the surrounding extracellular environment and can be divided into subgroups such as apoptotic bodies, microvesicles, and exosomes. It is difficult to standardize methods for isolating subgroups of EVs and procedures for purifying mixtures of vesicle types. Therefore, the International Society for Extracellular Vesicles has recently recommended the phrase “extracellular vesicle” as a generic term for isolated and studied vesicles when authors are unable to establish a specific marker.[12] Thus far, we have focused on medium- to large-sized (100–1000 nm) EVs in blood and urine to characterize EVs in healthy individuals.[13] Here, we found that urine from healthy individuals contains a large number of EVs expressing MUC1 on their surface, which could be derived from the tubular or uroepithelial surface of normal tissues.[13] We have also characterized EVs that are presumably derived from renal tubules that are positive for CD10, CD13, and CD26 (multipeptidase+ EVs).[13]

Although it remains difficult to use EVs as a diagnostic tool for UCB, a large body of evidence has accumulated demonstrating their potential as a biomarker for the noninvasive diagnosis of UCB.[14–16] Welton et al. analyzed urinary proteins in EVs and found that several proteins were elevated in UCB patients, including MUC1.[17]

In this study, we identified medium-sized uroepithelium-derived EVs in the urine of healthy subjects. We speculated that if cancerous uroepithelial cells were present, EVs distinguishable from those of healthy subjects might also be present in the urine of UCB patients. To characterize UCB EVs, we undertook a proteomic analysis of EV fractions extracted from UCB patients and searched for proteins that could serve as specific surface antigens.

2 | MATERIALS AND METHODS

2.1 | Patient specimens

Thirty-three human urine samples from 31 UCB patients and 18 human urine samples from 18 noncancerous patients that were obtained at Kyushu University Hospital between April 2019 and April 2022 were analyzed in this study. The patients' clinical information was obtained from their medical records. All patients provided written informed consent before undergoing the study procedures. Urine samples were also obtained from 29 healthy volunteers. The clinical protocol for this study was approved by the appropriate institutional review boards and ethics committees at Kyushu University Hospital. This study was carried out in accordance with the Declaration of Helsinki.

2.2 | Isolation of urinary mEVs

For the isolation of urinary EVs, we modified a urinary exosome extraction protocol.[18] We used a reduction process to degrade THP polymers and a centrifugation process to focus on medium-sized EVs with diameters ranging from 100 to 1000 nm.[13] In a flow cytometric analysis, the volume of urine used for each donor was approximately 10 ml (0.8 ml urine was used per assay, but approximately 10 ml was needed to combine single-stain assays for setting patient-specific compensation in multiple staining). In NTA, the volume of urine used per assay was 10 ml. Collected urine was centrifuged twice at 2330 *g* for 10 min. Once cells and large debris were removed, the urine supernatant was cryopreserved at −80°C. In the next protocol, the supernatant was thawed in a 37°C water bath and centrifuged at 2330 *g* to obtain the supernatant. The supernatant was centrifuged at 18,900 *g* for 30 min in a fixed-angle rotor. The EV pellet obtained from centrifugation was reconstituted by vortex mixing (1–2 min) with 0.2 ml DPBS followed by incubation with DTT (final concentration 10 mg/ml) at 37°C for 10–15 min. The samples were centrifuged again at 18,900 *g* for 30 min and the supernatant was discarded. Degraded THP monomers were removed from EVs after centrifugation. The DTT-containing DPBS solutions were filtered through 0.1-μm filters (Millipore Sigma).

2.3 | Nanoparticle tracking analysis

Nanoparticle tracking analysis measurements were carried out using a NanoSight NS300. All samples were diluted in PBS to a final volume of 0.8 ml. Concentrations were determined by pretesting the ideal particle per frame value (20–100 particles/frame). Extracellular vesicles labeled with ExoGlow-NTA Dye (System Biosciences), which binds specifically to intact EV membranes, were also measured by fluorescence NTA.[19–21] The settings of the device were in accordance with the manufacturer's software

manual (NanoSight NS300 User Manual, MAN0541-01-EN-00, 2017). Particles in the laser beam underwent Brownian motion and videos of these particle movements were recorded. NTA 3.2 software was then used to analyze the video and determine the particle concentration and the size distribution of the particles. Twenty-five frames per second were recorded for each sample with a "number of frames" setting of 1498. The detection threshold was 5 for both scattered light and fluorescence NTA. The detailed measurement parameters are shown in Supplementary Materials and Methods.

2.4 | Flow cytometric analysis of urinary EVs

After resuspending EV pellets in 60 μl DPBS, we added saturating concentrations of labeled Abs, annexin V, and normal mouse IgG, and incubated the tubes in the dark without stirring for 15–30 min at room temperature. Various Ab concentrations at the time of staining are listed in Supplemental Materials and Methods. We diluted this Ab-stained solution into 250 μl annexin V binding buffer (10 mM HEPES, 0.14 mM NaCl, 2.5 mM $CaCl_2$, pH 7.4; BD Biosciences), which was then subjected to flow cytometry analysis. The DPBS and annexin V binding buffer were filtered through 0.1-μm filters (Millipore). Flow cytometry was carried out using a FACSVerse flow cytometer (BD Biosciences). In our previous report, we implemented a method to measure particles smaller than 1 μm in size using polystyrene beads for verification and aggregating them into an observed image using side scatter.[13] The flow cytometer was equipped with 405 nm, 488 nm, and 638 nm lasers to detect up to 13 fluorescent parameters. The flow rate was 12 μl/min. Forward scatter voltage was set to 381, side scatter voltage was set to 340, and each threshold was set to 200. Details of excitation and emission wavelengths as well as voltages are described in the Supplementary Materials and Methods. Flow cytometry was carried out using FACSuite software (BD Biosciences) and data were analyzed using FlowJo software.

2.5 | Liquid chromatography–MS/MS analysis

Lysis of EVs and digestion of EV proteins prior to LC–MS/MS analysis were undertaken using the preparation method, as described previously[13] (Supplemental Materials and Methods). Digested peptides were dissolved in 25 μl 0.1% formic acid containing 2% (v/v) acetonitrile and 5 μl was injected into an Easy-nLC 1000 system (Thermo Fisher Scientific). Peptides were separated on an Acclaim PepMap RSLC column (15 cm × 50 μm inner diameter) containing C18 resin (2 μm, 100 Å; Thermo Fisher Scientific), and an Acclaim PepMap 100 trap column (2 cm × 75 μm inner diameter) containing C18 resin (3 μm, 100 Å; Thermo Fisher Scientific). The mobile phase consisted of 0.1% formic acid in ultrapure water (buffer A). The elution buffer was 0.1% formic acid in acetonitrile (buffer B); a linear 200 min gradient from 0%–40% buffer B was used at a flow rate of 200 nl/min. The Easy-nLC 1000 was coupled by a Nanospray Flex ion source (Thermo Fisher Scientific) to a Q Exactive Orbitrap (Thermo Fisher Scientific). The mass spectrometer was operated in data-dependent mode, in which a full-scan MS (from 350 to 1400 m/z with a resolution of 70,000, AGC 3E+06, maximum injection time 50 ms) was followed by MS/MS on the 20 most intense ions (AGC 1E+05, maximum injection time 100 ms, 4.0 m/z isolation window, fixed first mass 100 m/z, normalized collision energy 32 eV).

2.6 | Data interpretation

Proteome Discoverer 1.4 software (Thermo Fisher Scientific) was used for database searches. The database search was undertaken using the SequestHT algorithm using the *Homo sapiens* taxonomy catalogued in the UniProt database (UP000005640; October 18, 2020). Initial precursor mass tolerance was set at 10 ppm and fragment mass tolerance was set at 0.6 Da. Search criteria included static carbamidomethylation of cysteine (+57.0214 Da), dynamic oxidation of methionine (+15.995 Da), and dynamic acetylation (+43.006 Da) of lysine and arginine residues.

The obtained MS/MS data were further subjected to LFQ analysis using the MaxQuant platform (version 1.6.6.0). Database searches were carried out using the same UniProt database as described above. Digestion mode was set to Trypsin/P specificity, with a fixed carbamidomethyl modification of cysteine and variable modifications of protein N-terminal acetylation and methionine oxidation. Protein and peptide identification was undertaken under the following conditions: false discovery rate of 0.01, minimum number of peptides required for protein identification of 1, minimum score of 40 for modified peptides, and no lower limit for unmodified peptides.

Visualizations of the LFQ data were carried out using MetaboAnalyst 5.0 to identify specific proteins for UCB EVs (principal component analysis, heat map, and OPLS-DA). The evaluation of the model obtained by OPLS-DA was that the closer R2Y and Q2Y were to 1, the better the model; a model is considered good if R2Y is 0.65 or higher and Q2Y is 0.5 or higher.[22,23] Here, the proteins with variable importance in the projection (VIP) value greater than 1.0 were set for differential proteins. The VIP values larger than 1.0 point to the most relevant variables.[24,25] Gene enrichment analysis was carried out using Metascape.

2.7 | Statistical analysis

GraphPad Prism 9.2.0 (GraphPad Software) was used for the statistical analysis. Relationships between groups were compared using the Mann–Whitney *U*-test or Dunn's multiple comparison test (Kruskal–Wallis analyses were carried out). $p < 0.05$ was considered statistically significant.

3 | RESULTS

3.1 | Isolation of urinary mEVs and particle size distribution

To comprehensively recover all types of EVs without depending on the specificity of the membrane surface, we used a classical method of EV extraction by centrifugation (precipitated fraction by centrifugation at 18,900 *g*).[26,27] The precipitation fraction contains components with similar sedimentation coefficients and densities, except for EV. We treated the precipitated fraction with DTT to degrade and remove THP polymers that interacted with IgG.[13]

The extracted EV fractions were subjected to NTA using a Nanosight NS300.[28] Extracellular vesicles labeled with ExoGlow-NTA Dye, which specifically binds to the intact EV membrane, were also analyzed by fluorescence NTA.[21] Histograms of the particle size distributions of fractions extracted from healthy subjects and UCB patients, as measured by scattered light and fluorescence NTA, are shown in Figure 1A–D. The diameters corresponding to 10%, 50%, and 90% of the total number of particles observed by scattered light NTA in eight healthy subjects and eight UCB patients were compared (Figure 1E). In this enrichment operation, fractions with a diameter of 1 μm or more were rarely included, and the main fraction was distributed in the 200–300 nm diameter range. In addition, some of these fractions contained cell membranes (10%–60%), which were considered to be "mEVs" according to their size. The concentration in urine was calculated from the particle concentration detected in NTA. There were no differences in the particle size distribution or concentration of the extracted EV fractions between healthy subjects and UCB patients.

3.2 | Shotgun proteomic analysis of urinary EVs

Proteomic analysis using LC-MS/MS was undertaken to identify proteins specifically present in EVs in the urine of UCB patients.[29] Urine from four UCB patients (patient 1: Tis, urine cytology class III; patient 2: T2, urine cytology class V; patient 3: T2, urine cytology class V; patient 4: Ta, urine cytology class II) and four healthy subjects were used to enrich the EV fraction in urine. Two fractions were prepared: one was a mixed pool of samples from four patients and four healthy individuals, with the equivalent amount per patient after protein quantification for each group, and the other was an EV fraction extracted from each patient and one healthy individual. To gain an overview of the proteins contained in the urinary EVs of UCB patients, we first undertook a shotgun analysis of the pooled samples. The proteins detected in each of the two groups were selected from the Proteome Discoverer search results with a score of 1.0 or higher. These proteins are shown in a Venn diagram in Figure 2A and are listed in the Data S1. Enrichment analysis using Metascape was carried out on the proteins detected in UCB patients only (585 proteins) (Table 1). Although there were some functional categories related to cell adhesion, which is a characteristic of cancer, the most frequently categorized functions of proteins included eukaryotic translation elongation and ribonucleoprotein complex assembly RNA. Ribosome-related functional categories (protein complex, translation) were calculated. This could be one feature of the proteins contained in EVs derived from cancer patients.

The analysis was undertaken using individually extracted EVs. The obtained MS/MS data were subjected to LFQ analysis using the MaxQuant platform, and the quantitative results for each patient were calculated.[30,31] In the analysis of extracted EV fractions from four healthy subjects and four UCB patients, 1957 different proteins were detected (Data S1). MetaboAnalyst 5.0 was used for the statistical analysis. Principal component analysis was undertaken from the results of each of the four UCB patients and four healthy subjects (Figure 2B). Although Patient 2 had a slightly different profile to the other three patients, there were some differences in the detected protein profiles between the groups of four UCB patients and four healthy individuals. We carried out OPLS-DA analysis, which allows discriminant analysis between groups. In the score plot shown in Figure S1, R2X = 0.253, R2Y = 0.847, and Q2Y = 0.608. Because R2Y and Q2Y were good, the patient group and the healthy group were significantly discriminated. Next, screening was carried out using and VIP values and S-plot to identify key markers that differentiate UCB from healthy subjects. Those with a large contribution to the discrimination of the two groups and an increase in UCB were extracted from the s-plot, and those with a VIP value exceeding 1.0 were selected (Data S1). A heat map of the 64 proteins extracted by this analysis was used to separate the healthy group from the patient group by clustering (Figure 2C). Of the 64 selected proteins, 31 proteins, or approximately half, were categorized as both "plasma membrane" and "extracellular exosome" in Gene Ontology (AGRN, ANXA2, APOA1, APOB, C3, C9, CEACAM5, CFB, CP, F2, FAM129B, FGB, FGG, FN1, IGHA1, IGHG1, IGHG2, IGHM, IGKC, MARCKS, PLG, PROS1, PSCA, RAB27B, SDCBP2, SERPINC1, SLC2A1, SRC, TACSTD2, TF, and UPK3A). Proteins that have been reported to be upregulated in UCB (UPK3A, PSCA, ANXA2, and ANXA9) were included,[32–34] indicating the validity of the analysis.

We found several proteins that are increased in UCB, but we needed to select among these for diagnostic applications, that is, membrane proteins that can detect EVs from the outside. Proteins that contribute to the grouping of patients and healthy subjects include CEACAM5 and CEACAM7, and we wondered whether these could characterize EVs from the outside in light of this point. The profiles of all detected CEACAM family proteins are shown in the heat map (Figure 2D) and comprised CEACAM1 (CD66a), CEACAM5 (CD66e), CEACAM6 (CD66c), CEACAM7 (CGM2), and CEACAM8 (CD66b). Although the expression profiles of these CEACAM proteins differed among patients, they shared a common increasing trend in patients. The expression profiles of these five CEACAMs are shown in the Human Protein Atlas, which shows strong staining for CEACAM5, CEACAM6, and CEACAM7, especially in the tissues of patients with urothelial cancer.

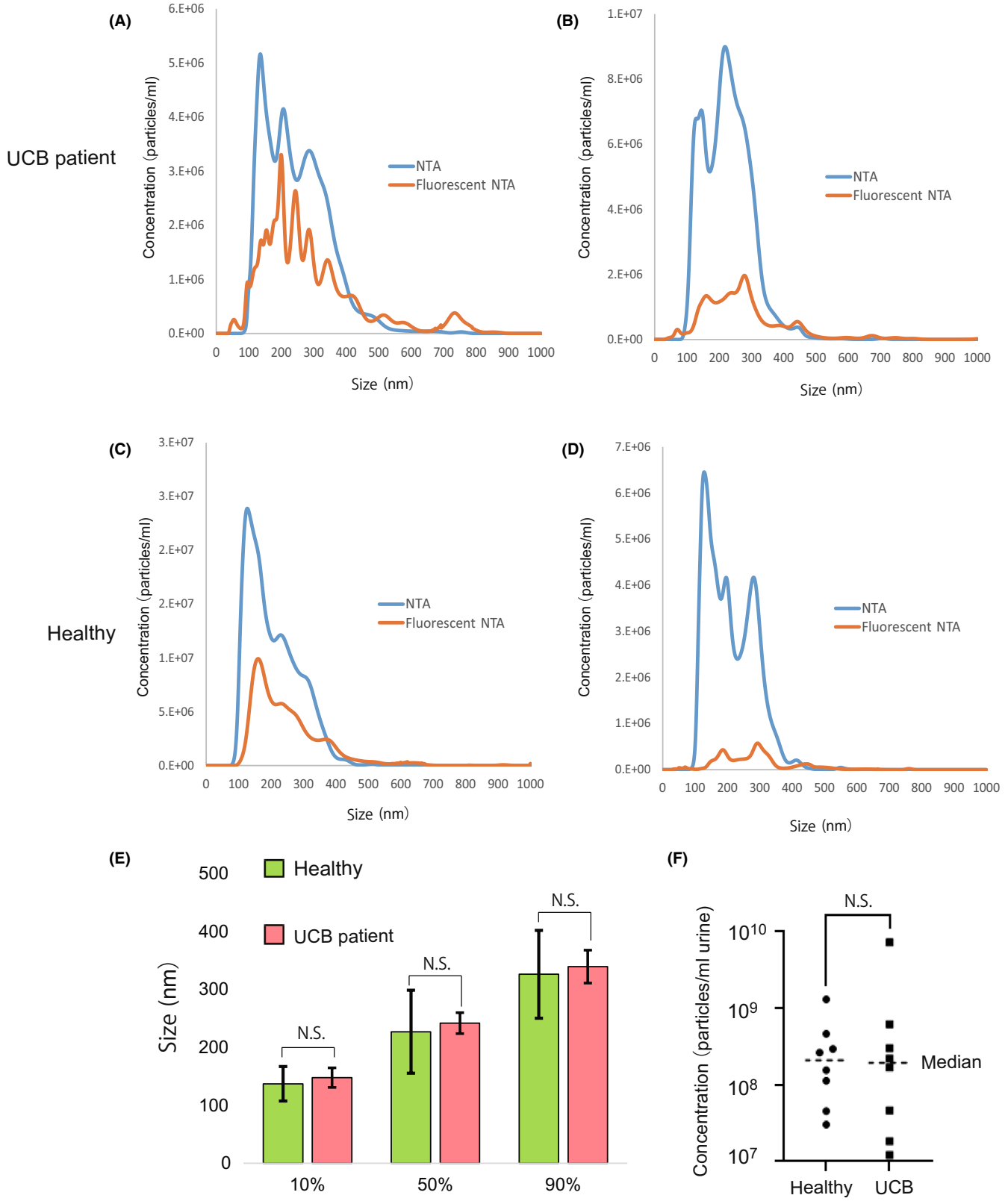

FIGURE 1 Particle size distribution of fractions extracted from urine by nanoparticle-tracking analysis (NTA). Blue and orange lines indicate the particle size distribution by scattered light and fluorescence, respectively. Fluorescent NTA is an image obtained from a particle with a lipid bilayer. (A, B) Examples of patients with urothelial carcinoma of the bladder (UCB). (C, D) Examples of healthy subjects. (E) Comparison of the particle size distributions at the 10th, 50th, and 90th tiles of the total particle size distributions of eight UCB patients and eight healthy subjects, using scattered light measurement. (F) Comparison of detected particle concentrations per urine between UCB patients and healthy subjects. Significance was determined by Mann–Whitney test. N.S., not significant

3.3 | Characterization of urinary EVs expressing CEACAM proteins by flow cytometry

Among the selected proteins that were upregulated in UCB, there was a limited number expressed in the plasma membrane that could be used for characterization as mEVs, and we considered CEACAMs to be prime candidates. A subgroup of the CEA family, CEACAMs are found in a range of different cell types and organs.[35] They are involved in a number of different processes including cell adhesion, proliferation, differentiation, and tumor suppression.[36] Some CEACAMs, such as CEACAM1, CEACAM5, and CEACAM6, are highly associated with cancer.[7,36–38] As each of these CEACAM antigens has its own characteristics, we examined whether the localization of these antigens and their internalization into EVs differed from patient to patient. The urine of nine UCB patients was analyzed using the flow cytometric technique described above. In Patient 1 (UCB1), the EVs positive for CD66a, CD66c, and CD66e merged with those positive for other antigens (Figure 3A). This patient had EVs expressing all three antigens simultaneously on their surface. In UCB3, we identified a large number of EVs positive for CD66a only. In UCB4, we found EVs in which CD66e and CD66a were merged and EVs in which CD66a was present alone. Next, urine from nine UCB patients was analyzed by flow cytometry. The percentage of EVs that were positive for each of the individual antigens CD66a, CD66c, and CD66e and the percentage of EVs that were positive for each of the antigens that merged are shown in the graph of the results for nine patients (Figure 3B). This result suggests that each patient had a different variety of EVs that were positive for CD66a, CD66c, and CD66e. The presence of EVs that were positive only for CD66a, CD66c, and CD66e alone, or that had two or three of these antigens present simultaneously, was suggested. Patient 2 showed CEACAM8 in shotgun analysis; therefore, we attempted to detect it by flow cytometry and were able to observe CEACAM8-positive EVs (Figure S2). However, in flow cytometry analysis, the EVs in which CEACAM8 expression could be observed were infrequent in patient urine. We also observed a population of EVs that merged with CD66a/CD66c/CD66e, suggesting that the EVs were simultaneously expressing one of these antigens.

Because many EVs with major CD66a, CD66c, and CD66e (CEACAM1, CEACAM6, and CEACAM5) were observed in the patient's urine, we decided that a measurement system using an Ab that recognizes these antigens without distinction would be appropriate, and conducted a flow cytometric analysis using this Ab (Clone ASL-32). Figure 3C shows a typical example. This is in order to achieve a more sensitive diagnostic system. Extracellular vesicles that were CD66a-/CD66c-/CD66e-positive by Clone ASL-32 (CEACAM+ EVs) were selected after gating to remove multiple aggregated particles, to remove particles reactive to IgG (e.g., THP polymer), and to distinguish them from multipeptidase+ EVs derived from renal tubules (Figures 3D and S3).

The CEACAM+ EVs were also MUC1-positive EVs (Figures 3E and S3), although many MUC1+ EVs were detected in the urine of healthy individuals. It is possible that CEACAM+ EVs were originally derived from uroepithelial cells and secreted with CEACAM family proteins on their surface as antigenic.

We also observed the nature of the lipid bilayer in CEACAM+ EVs with annexin V (exposure of PS). Phosphatidylserine appeared to be facing out of EV membranes to varying degrees, depending on the patient (Figure S4).

3.4 | Verification of possible diagnostic applications of CEACAM+ EVs using urine from UCB patients

Erythrocyte-derived EVs were present in the urine of hematuric patients (Figure S3). Multipeptidase+ EVs derived from renal tubules were characterized in the same way as in previous studies (Figure S3).[13] In the flow cytometric analysis, there were four types of EVs in patients' urine that could be characterized on the basis of our previous studies[13]: (i) MUC1+ uroepithelial EVs (CD66a-/CD66c-/CD66e-negative); (ii) CEACAM+ EVs; (iii) multipeptidase+ EVs derived from renal tubules; and (iv) erythrocyte-derived EVs (Figure 4A).

We confirmed that CEACAM+ EVs were not abundant in the urine of healthy subjects and non-UCB patients (Figure 4B). Therefore, 33 UCB urine specimens, 18 non-UCB (urological disease) specimens, and 29 healthy specimens, all from men, were used to analyze the four types of EVs by the characterization method described above using a flow cytometer (Table 2, Figure S5). The proportion (%) of these four types of EVs observed in the urine in the entire image is shown in Figures 4C and S6. The number of CEACAM+ EVs was significantly increased in UCB (mean ± SD, 8.6% ± 13%) compared to non-UCB (0.69 ± 0.46) and healthy (0.46 ± 0.34) (Figure 4D). The number of MUC1+ EVs was slightly decreased in UCB (10 ± 5.8) compared to non-UCB (16 ± 8.5) and healthy (17 ± 9.0) (Figure 4D). The number of multipeptidase+ EVs was also slightly decreased in UCB (26 ± 19) compared to healthy (38 ± 14) (Figure 4D). The present

FIGURE 2 Shotgun proteomic analysis of urine extracellular vesicles (EVs) from patients with urothelial carcinoma of the bladder (UCB). (A) Venn diagram showing the number of proteins identified by analyzing pooled samples from four patients and four healthy subjects each. (B) Label-free quantification data of 1957 proteins from the four UCB patients and four healthy subjects were subjected to principal component (PC) analysis. (C) Orthogonal partial least squares discriminant analysis was undertaken on the same data as in (B). Proteins that significantly contributed to the grouping in this analysis and showed an increase in the patient group were extracted, and these are shown in the heat map. Proteins that are categorized as both "plasma membrane" and "extracellular exosome" in Gene Ontology are shown in green. Extracted carcinoembryonic antigen-related adhesion molecule (CEACAM) proteins are circled in pink. (D) All of the CEACAM family proteins detected in the analysis were compared by heat mapping in patients and healthy subjects

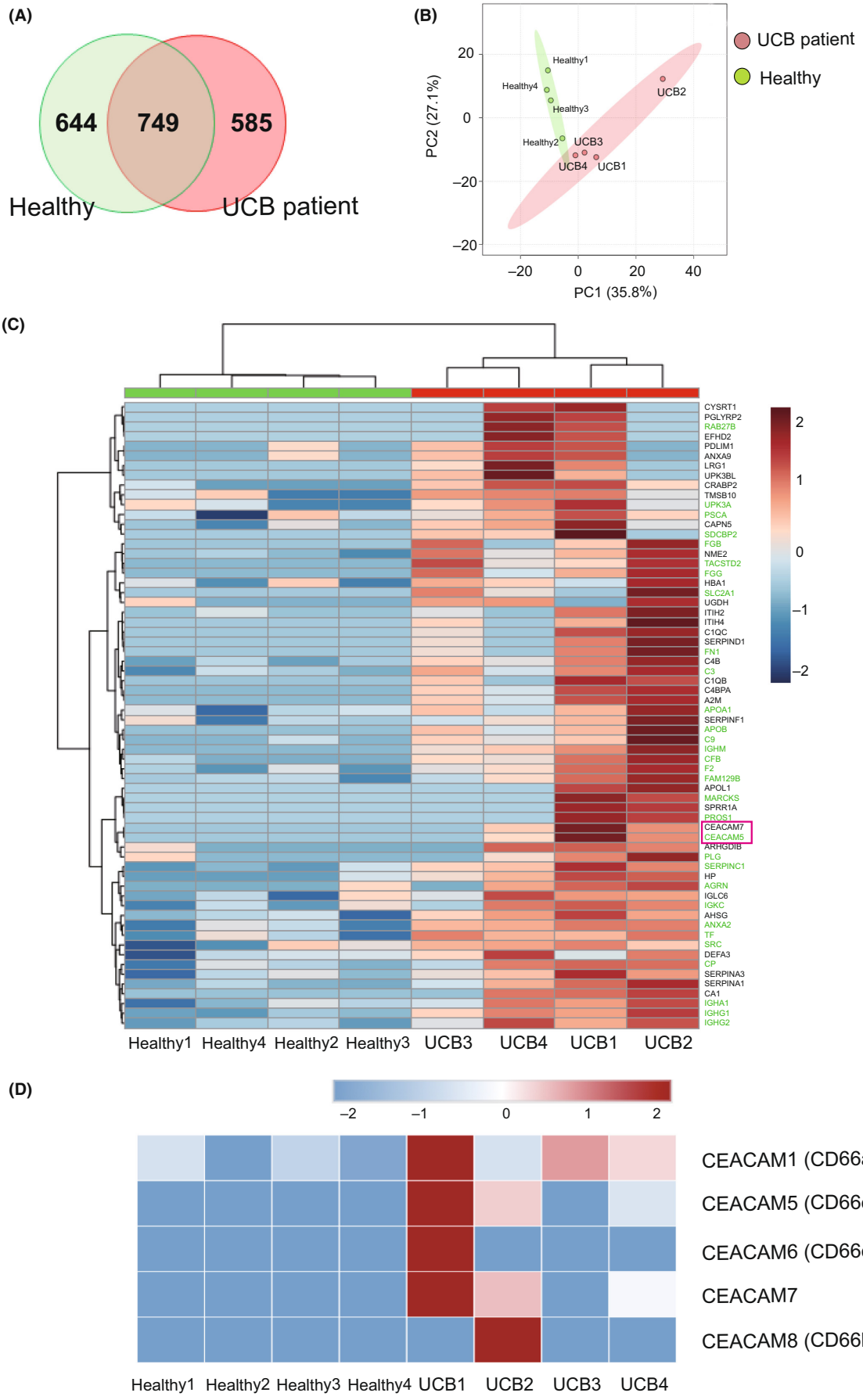
(A)
644
749
585
Healthy
UCB patient
(B)
UCB patient
Healthy
PC2 (27.1%)
PC1 (35.8%)
Healthy1
Healthy4
Healthy3
Healthy2
UCB3
UCB4
UCB1
UCB2
(C)
CYSRT1
PGLYRP2
RAB27B
EFHD2
PDLIM1
ANXA9
LRG1
UPK3BL
CRABP2
TMSB10
UPK3A
PSCA
CAPN5
SDCBP2
FGB
NME2
TACSTD2
FGG
HBA1
SLC2A1
UGDH
ITIH2
ITIH4
C1QC
SERPIND1
FN1
C4B
C3
C1QB
C4BPA
A2M
APOA1
SERPINF1
APOB
C9
IGHM
CFB
F2
FAM129B
APOL1
MARCKS
SPRR1A
PROS1
CEACAM7
CEACAM5
ARHGDIB
PLG
SERPINC1
HP
AGRN
IGLC6
IGKC
AHSG
ANXA2
TF
SRC
DEFA3
CP
SERPINA3
SERPINA1
CA1
IGHA1
IGHG1
IGHG2
Healthy1 Healthy4 Healthy2 Healthy3 UCB3 UCB4 UCB1 UCB2
(D)
CEACAM1 (CD66a)
CEACAM5 (CD66e)
CEACAM6 (CD66c)
CEACAM7
CEACAM8 (CD66b)
Healthy1 Healthy2 Healthy3 Healthy4 UCB1 UCB2 UCB3 UCB4

results also showed no association between aging and the proportion (%) of CEACAM+ EVs (Figure S5).

The diagnostic performance was evaluated by ROC curve in UCB and others (non-UCB and healthy specimens) (Figure 4E). The area under the ROC curve was 0.907 (95% confidence interval, 0.833–0.981; $p < 0.0001$). On the basis of these results, the provisional cut-off point was also calculated, taking into account both sensitivity (81.82%) and specificity (97.87%).

The provisional CEACAM+ EVs percentage cut-off value was 1.34%. Twenty-nine urine samples from patients with UCB were compared for the results of urine cytology (class 2–5) and the overall percentage of CEACAM+ EVs in this method. The results of urine

TABLE 1 Gene enrichment analysis of proteins in urine-derived extracellular vesicle fractions from patients with urothelial carcinoma of the bladder, by Metascape

Category	Description	Count[a]	%[b]	$Log_{10}(p)$[c]
Reactome	Eukaryotic translation elongation	39	7.0	−41.0
KEGG	Complement and coagulation cascades	33	5.9	−34.6
GO	**Regulated exocytosis**	73	13	−27.7
Reactome	**Hemostasis**	55	9.8	−19.7
GO	Activation of immune response	58	10	−18.0
GO	Extracellular structure organization	43	7.7	−16.4
GO	Integrin-mediated signaling pathway	20	3.6	−13.4
GO	Blood coagulation, fibrin clot formation	12	2.1	−13.1
GO	Regulation of peptidase activity	37	6.6	−12.2
CORUM	DGCR8 multiprotein complex	8	1.4	−11.4
GO	Cell junction organization	29	5.2	−10.9
Wiki	VEGFA–VEGFR2 signaling pathway	34	6.1	−10.8
GO	Regulation of cell adhesion	45	8.0	−10.5
Reactome	**Transport of small molecules**	43	7.7	−9.6
GO	Leukocyte migration	35	6.3	−9.5
GO	Ribonucleoprotein complex assembly	25	4.5	−9.4
Reactome	Regulation of insulin-like growth factor transport and uptake by insulin-like growth factor binding proteins	17	3.0	−9.3
GO	Fibrinolysis	9	1.6	−9.2
GO	Heterotypic cell–cell adhesion	12	2.1	−8.6
Wiki	mRNA processing	16	2.9	−8.4

Note: Top 20 clusters with their representative enriched terms (one per cluster). Categorization was carried out with the following ontology sources: CORUM; GO, Gene Ontology Biological Processes; KEGG, Kyoto Encyclopedia of Genes and Genomes Pathway; Reactome, Reactome Gene Sets; and Wiki, Wiki Pathways. Descriptions in bold are those also calculated for urine-derived EV fractions from healthy subjects.

Abbreviations: VEGFA, vascular endothelial growth factor A; VEGFR2, VEGF receptor 2.

[a]Number of genes in the user-provided lists with membership in the given ontology term.

[b]Percentage of all the user-provided genes that were found in the given ontology term (only input genes with at least one ontology term annotation are included in the calculation).

[c]*p* Value in log base 10.

FIGURE 3 Characterization of extracellular vesicles (EVs) in urine of patients with urothelial carcinoma of the bladder (UCB) by flow cytometry. (A) Antibodies that recognize CD66a, c, and e antigens, are used to evaluate the properties present in EVs. Patient 1: three antigens are expressed simultaneously. Patient 2: only CD66a is expressed. Patient 4: simultaneous expression of CD66a and e, expression of CD66a alone. (B) EVs that are positive for CD66a, c, and e, and EVs in which each antigen is merged were evaluated in nine patients. CD66a-c merged indicates the fraction where CD66a and CD66c positivity merge. The upper panel shows the percentages of each EV in the entire image, and the lower panel shows the percentages of each EV when CD66a is set to 100%. (C) Observation of EVs that are specifically positive in the urine of patients using Ab (Clone ASL-32) that simultaneously recognize CD66a, c, and e without distinction. (D) Comparison of CD66a/c/e-positive (carcinoembryonic antigen-related adhesion molecule [CEACAM]+) and CD26-positive fractions in observation images. CEACAM+ EVs are different from multipeptidase-positive (CD26-positive) EVs derived from renal tubules. (E) Comparison of the CEACAM+ and MUC1-positive fractions in images. Fractions in which each fraction merged and fractions in which only MUC1 was positive were observed

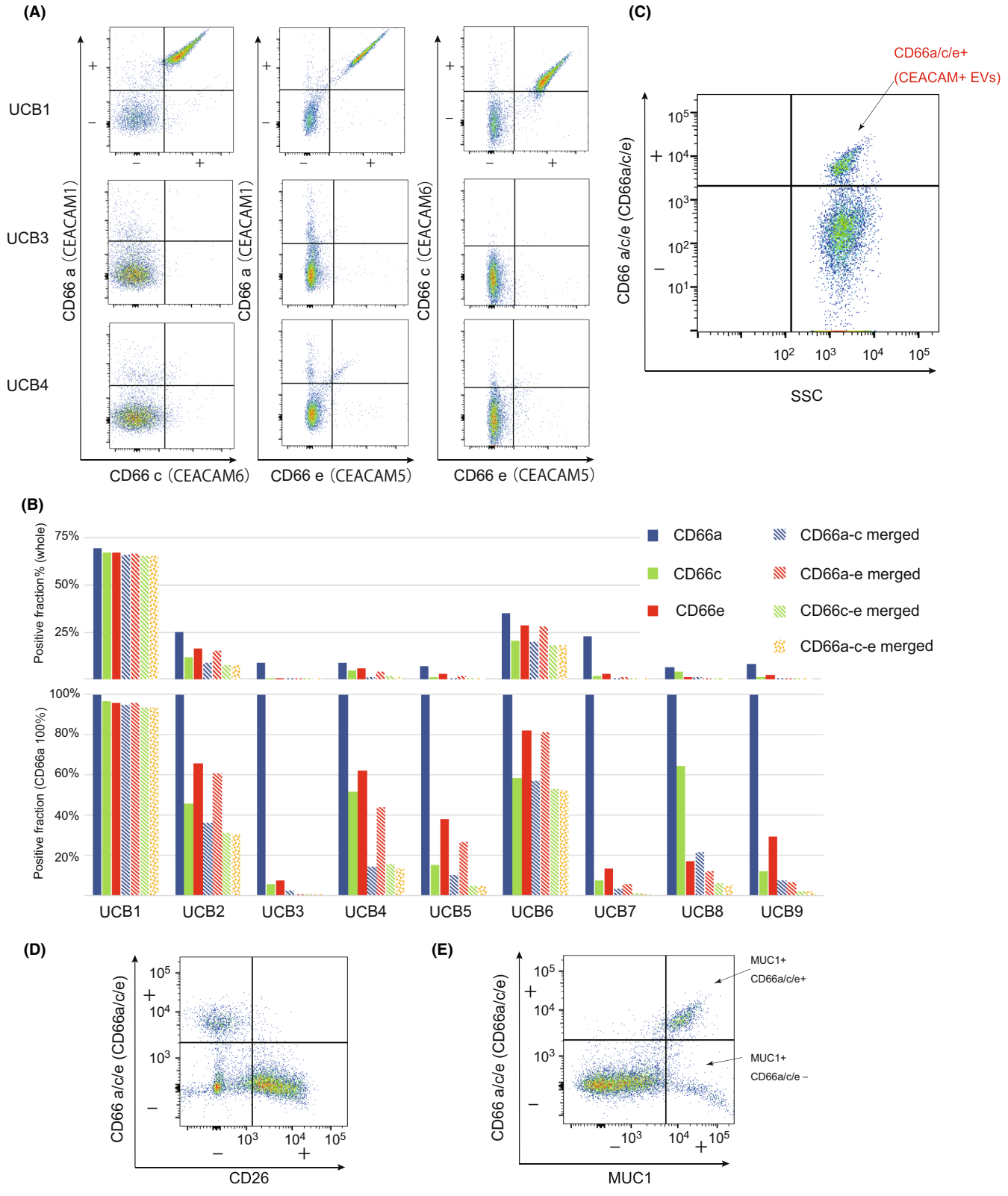

cytology of UCB were: class 2, nine cases; class 3, six cases; class 4, two cases; and class 5, 12 cases (Table 2). Using this method, seven of the nine cases with urine cytology results in class 2 (negative) were judged as positive (Figure 4F). This suggests that the method covers the oversights of existing urine cytology and could be implemented as a valid test.

4 | DISCUSSION

The release of microvesicles or microparticles (in other words, mEVs) by tumor cells is a very common event in the tumor microenvironment.[39] As a result, tumor-derived mEVs not only influence tumor cell biology but also profoundly advance tumor immunology.[40,41]

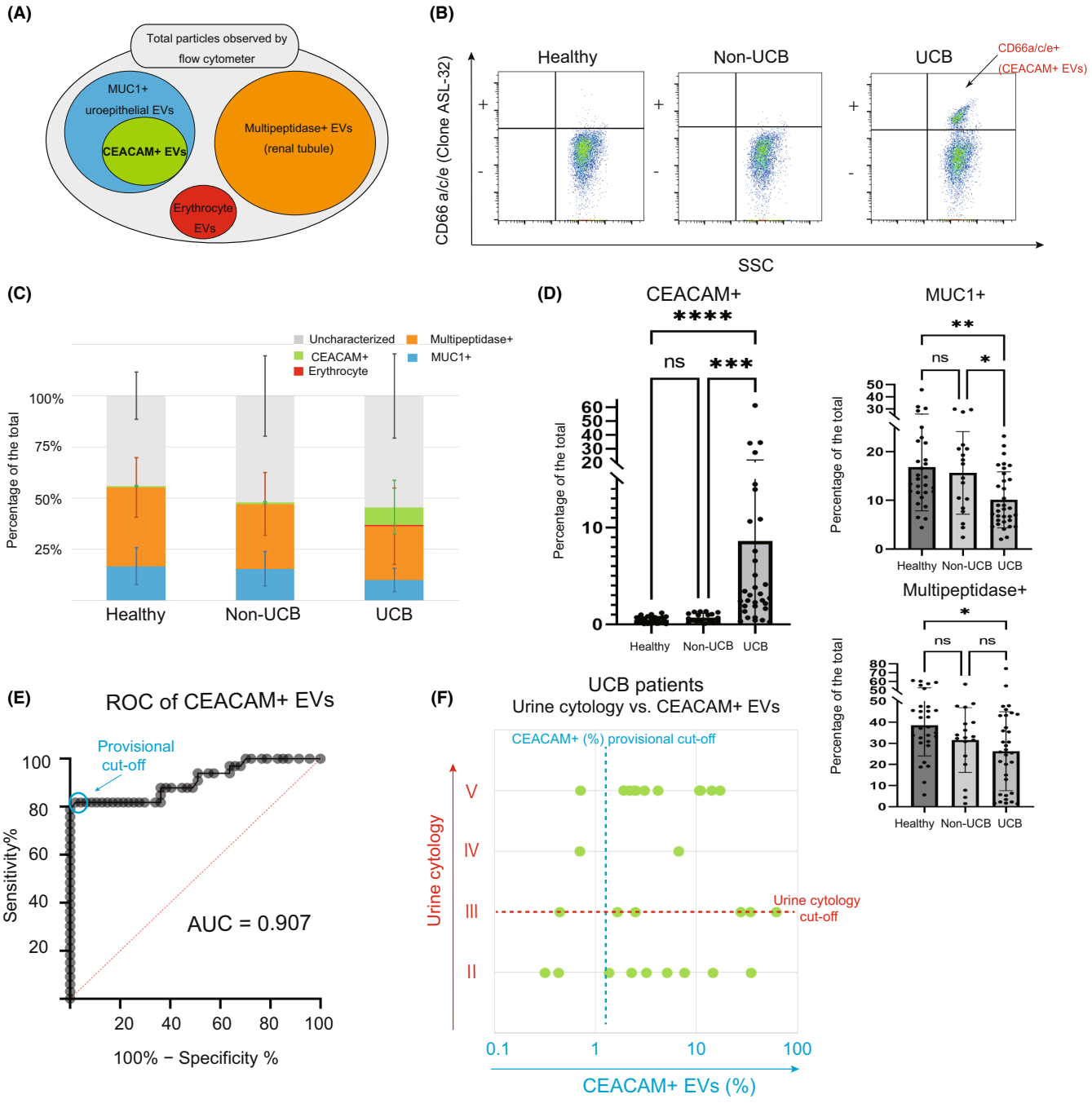

FIGURE 4 Evaluation of flow cytometric analysis of extracellular vesicles (EVs) in urine as a diagnostic method for urothelial carcinoma of the bladder (UCB). (A) Schematic diagram of EVs that can be characterized in the observation area using urine from a UCB patient. (B) ASL-32 Ab staining of EVs extracted from urine of healthy subjects, noncancer patients, and UCB patients, showing CD66a/c/e-positive fractions. (C) Healthy specimens ($n = 29$), noncancer specimens ($n = 18$), and UCB specimens ($n = 33$) were characterized by flow cytometry, and the mean values of the percentages of particles in the observed images of four fractions (mucin 1 [MUC1]+, carcinoembryonic antigen-related adhesion molecule [CEACAM]+, Multipeptidase+ and Erythrocyte) are shown in a stacked graph. (D) Comparison of CEACAM+, MUC1+, and Multipeptidase+ fractions. Box indicates mean value and error bars indicate SD. (E) Results of this measurement for the 33 UCB specimens and the noncancer group (18 noncancer specimens + 29 healthy specimens) are shown in the receiver operating characteristic (ROC) curve. Based on the results, a provisional cut-off point is set with a blue circle. (F) Comparison of urine cytology results with CEACAM+ EVs in cancer patients.[29] The cut-off value for urine cytology was III; the cut-off for CEACAM+ EVs was 1.3%, the same as in (D). Significance was determined by Dunn's multiple comparison test. *, $p < 0.05$; **, $p < 0.01$;***, $p < 0.001$;****, $p < 0.0001$. AUC, area under the ROC curve; ns, not significant

TABLE 2 Disease status and percentage of carcinoembryonic antigen-related adhesion molecule [CEACAM]+ extracellular vesicles (EVs) in 33 urothelial carcinoma of the bladder (UCB) specimens

	Age (years)			T stage	Grade	Urine cytology	CEACAM+ EVs %
UCB1	75	Urothelial carcinoma	Recurrent	Tis	High	III	61.0
UCB2	58	Urothelial carcinoma	Recurrent	T2	High	V	17.0
UCB3	70	Urothelial carcinoma	Primary	T2	High	V	1.9
UCB4	84	Urothelial carcinoma	Primary	Ta	Low	II	3.2
UCB5	67	Urothelial carcinoma	Recurrent	Tis	High	V	2.5
UCB6	71	Urothelial carcinoma	Recurrent	T1	High	III	27.0
UCB7	64	Urothelial carcinoma	Primary	Ta	Low	II	5.1
UCB8	69	Urothelial carcinoma	Primary	T1	High	V	2.4
UCB9	69	Urothelial carcinoma	Recurrent	T1	High	II	14.0
UCB10	52	Urothelial carcinoma	Primary	T2	High	V	3.0
UCB11	52	Urothelial carcinoma	Primary	T2	High	V	14.0
UCB12	77	Urothelial carcinoma	Recurrent	T2	High	III	34.0
UCB13	91	Urothelial carcinoma	Recurrent	T2	High	V	11.0
UCB14	63	Urothelial carcinoma	Primary	T2	High	V	0.7
UCB15	64	Urothelial carcinoma	Primary	Ta	Low	II	0.4
UCB16	75	Urothelial carcinoma	Primary	T1	High	IV	0.7
UCB17	57	Urothelial carcinoma	Primary	Ta	Low	II	34.0
UCB18	84	Urothelial carcinoma	Primary	Ta	Low	II	1.3
UCB19	70	Urothelial carcinoma	Recurrent	T1	High	II	2.3
UCB20	73	Urothelial carcinoma	Primary	Ta	Low	III	0.4
UCB21	62	Urothelial carcinoma	Primary	Ta	High	III	2.5
UCB22	89	Urothelial carcinoma	Primary	T1	High	IV	6.6
UCB23	75	Urothelial carcinoma	Primary	T1	High	V	1.9
UCB24	61	Urothelial carcinoma	Primary	T1	High	V	2.1
UCB25	64	Urothelial carcinoma	Primary	Ta	Low	II	7.6
UCB26	64	Urothelial carcinoma	Primary	Ta	Low	III	1.6
UCB27	68	Urothelial carcinoma	Primary	T1	High	V	4.1
UCB28	85	Urothelial carcinoma	Primary	T1	High	V	11.0
UCB29	67	Urothelial carcinoma	Primary	Ta	Low	II	0.3
UCB30	72	Urothelial carcinoma	Primary	T2	High	– (*)	3.8
UCB31	64	Urothelial carcinoma	Primary	Ta	Low	– (*)	2.7
UCB32	84	Urothelial carcinoma	Recurrent	T1	High	– (*)	3.4
UCB33	63	Urothelial carcinoma	Primary	Ta	Low	– (*)	0.2

– (*), no urine cytology measurement on the same sample.

The described methods for mEV isolation include step-wise centrifugation, which removes large cellular debris, followed by ultracentrifugation (14,000*g*) to pellet the mEVs.[42] A method to observe tumor-derived mEVs in blood by flow cytometry was also introduced.[43] We extracted EV fractions from urine by centrifugation at 18,900*g*. From the results of NTA, particle size fractions with a diameter of approximately 300 nm were mainly extracted from both healthy subjects and patients.

From the fluorescence NTA results, we also observed that the extracted fractions contained particles with lipid-bilayer membranes. In addition, there are reports that blood cell-derived mEVs express PS and are related to cancer malignancy,[44,45] but there are also reports that tumor-derived mEVs express PS.[46] In Figure S4, we observed that some CEACAM+ EVs were positive for annexin V. These might be involved in some cancer characteristics, as described above.[46]

In the shotgun proteomic analysis of pooled samples of patients and healthy controls, a large number of ribosome-related functional proteins were detected in the fraction specifically extracted from UCB. These could include rRNA and other RNAs, especially cancer-derived EVs. RNA profiles in EVs released into culture medium have been analyzed by experiments undertaken in cell lines.[47,48] Crescitelli et al. also profiled RNA in EVs extracted from melanoma

tissue.[49] In the future, nucleic acid content could become a new cancer biomarker by analyzing RNA in UCB EVs.

In an individual analysis of four healthy subjects and four UCB patients, we were able to select proteins that contributed to each grouping and were particularly increased in the patient groups. These selected proteins could be potential biomarkers specific to UCB because their dynamics can be divided into two groups in healthy subjects and patients by clustering (Figure 2C), and some proteins have been reported to be increased in UCB. Many of the extracted proteins are adjacent to the plasma membrane, and annexins are an example of such proteins. Recently, the expression of annexin family members in UCB tissues was reported in detail.[34] In this report, ANXA2, ANXA3, ANXA4, ANXA8, and ANXA9 were significantly increased in UCB tissues, consistent with our results showing the upregulation of ANXA2 and ANXA9. UPK3A is said to be present in apical plasma membrane urothelial plaques, and there are reports of its very good diagnostic performance, especially when measured by ELISA in urine.[32] Our results also show that UPK3A is increased in patients; thus, focusing on UPK3A-expressing EVs in urine could be a new diagnostic approach.

In the OPLS-DA analysis, CEACAM5 and CEACAM7 were selected as important components for discrimination, and CEACAM1, CEACAM6, and CEACAM8 were also detected, all of which have an increasing trend in UCB patients. These CEACAM proteins other than CEACAM1 were detected by immunostaining of UCB tissues in The Human Protein Atlas, which showed medium to high levels of expression. Tilki et al. demonstrated by immunostaining that the percentage of CEACAM1 expression in tumor-associated vessels increases with advancing tumor stage and that patients with invasive UCB express CEACAM1 in tumor-associated vessels.[7] In this study, we found that CEACAM proteins, which were increased in the EV fraction of UCB patients, were also upregulated in UCB tissues.

To characterize UCB-specific mEVs by flow cytometry, it was necessary to evaluate the expression distribution of CEACAM proteins. Muturi et al. found that CEACAM1, CEACAM5, and CEACAM6 are present in mEVs derived from cancer epithelial cells and vascular endothelial cells.[50] Zheng et al. also suggested that CEACAM1 and CEACAM5 could be used to characterize exosomes in the duct fluid of pancreatic cancer patients.[51] These reports suggest that there could be multiple types of CEACAM proteins in EVs. Our results show that CEACAM1, CEACAM5, and CEACAM6 are present in mEVs with various patterns of expression in different patients. If CEACAM family proteins are expressed as differentiation antigens, it would be interesting to see how they relate to patient conditions. We believe that this is an issue for future large-scale clinical studies. Mucin 1 is present in the bladder tissue of healthy individuals (The Human Protein Atlas) and was identified in EVs in the urine of healthy individuals in our study, suggesting that it might characterize EVs derived from the uroepithelium.[13] In our results, CEACAM+ EVs were also MUC1+. Thus, CEACAM+ EVs may result from the secretion of CEACAM family proteins on the surface of cells that were originally derived from uroepithelial cells and that became cancerous as part of their antigenic properties.

Although the number of urine-derived EVs varies from patient to patient, in this study, their diagnostic performance was evaluated according to the percentage of CEACAM+ EVs in the particles observed in flow cytometry measurements. In their review, Oeyen et al. introduced the sensitivity and specificity of various FDA-approved urine-based tests for UCB, but these tests do not replace urine cytology or cystoscopy because of their poor diagnostic performance and problems with false positives.[6] These kits have a mean sensitivity not exceeding 80%, and false positives resulting from hematuria have been a problem. In our system, erythrocyte-derived EVs originating from hematuria can be measured separately, and thus any resulting nonspecific reactions and false positives are not a problem. The clinical sensitivity must be verified by large-scale clinical studies, but we believe that our system also requires improvement. Tilki et al. reported clinical sensitivity of 74% (69/93) and specificity of 95% (40/42) for measurement using CEACAM1 in urine,[7] and our results were close to this. In addition to CEACAM proteins, shotgun proteomics analysis revealed several proteins that could be potential markers for UCB in EVs, and we would like to further examine the possibility of improving sensitivity by combining these proteins. Urothelial carcinoma of the bladder has a high recurrence rate, and prognostic monitoring tests in the postoperative or treatment course are very important. The urine samples examined in this study, including those from patients who presented with recurrence after transurethral resection of bladder tumor and during treatment, had a high number of CEACAM+ EVs (>10%) (Table 2). It is necessary to verify these findings in the future, along with the elucidation of the generation mechanism of CEACAM+ EVs and their relationship with cancer progression.

In this study, we used flow cytometry for mEV measurement to detect multiple antigens and to confirm a certain particle size. Considering the actual specimen processing and testing, the application of a simple automated assay system is desirable. An assay system that can directly measure exosomes in body fluids without EV extraction was recently reported. One is ExoScreen (Theoria Science, Inc.), which targets smaller EVs (e.g., exosomes) and could be implemented for biomarker screening in a variety of diseases.[52] Another system, ExoCounter (JVCKENWOOD Corporation), can determine the exact number of exosomes in the serum of cancer patients.[53] These have potential applications in automated systems that can process large numbers of specimens, but at present, both systems are limited to EVs with a size of 200 nm or less, and thus they need to be improved before their application to CEACAM+ EVs. Furthermore, EV detection technology has advanced rapidly in recent years, and their application to better measurement systems is expected.[54,55] Extracellular vesicles expressing CEACAM proteins in the urine of UCB patients could form a new liquid biopsy test. In the future, we aim to improve this protocol to make it easier and more practical, as well as to deepen the analysis of EV contents to expand the possibilities of liquid biopsies.

ACKNOWLEDGMENTS

We thank the laboratory members of Clinical Chemistry and Laboratory Medicine, Kyushu University, for reagents, discussions, and carefully reviewing the manuscript. We would like to express our gratitude to the Department of Urology and Laboratory Medicine, Kyushu University, for collecting valuable clinical samples. We are grateful to LSI Medience Corporation for its generous support during this study. This research was supported by Grants-in-Aid for Scientific Research from the Japan Society for the Promotion of Science (grant numbers 17H01550, 18K15421, and 20H00530) and AMED (grant number JP21lm0203009). Finally, we thank H. Nikki March, PhD, from Edanz for editing a draft of this manuscript.

CONFLICT OF INTERSET

K. Igami is a full-time employee of LSI Medience Corporation. K. Igami is also seconded to and belongs to Kyushu Pro Search Limited Liability Partnership, a subsidiary of LSI Medience Corporation. M. Eto is an Editorial Board Member of *Cancer Science*. No disclosures were reported by the other authors.

CLINICAL TRIAL REGISTERATION INFORMATION

This study was approved by the Clinical Research Ethics Review Committee of the Department of Medicine, Kyushu University, with permission number 2019–063.

ORCID

Takeshi Uchiumi https://orcid.org/0000-0002-3665-233X
Masaki Shiota https://orcid.org/0000-0002-3306-4858
Shigehiro Tsukahara https://orcid.org/0000-0002-3533-6781
Masatoshi Eto https://orcid.org/0000-0002-3312-9930

REFERENCES

1. Jemal A, Siegel R, Ward E, Hao Y. Cancer statistics. *CA Cancer J Clin*. 2008;58(2):71-96.
2. Rahib L, Wehner MR, Matrisian LM, Nead KT. Estimated projection of US cancer incidence and death to 2040. *JAMA Netw Open*. 2021;4(4):1-14.
3. Zieger K, Wolf H, Olsen PR, Højgaard K. Long-term follow-up of noninvasive bladder tumours (stage ta): recurrence and progression. *BJU Int*. 2000;85(7):824-828.
4. Witjes JA, Hendricksen K. Intravesical pharmacotherapy for non-muscle-invasive bladder cancer: a critical analysis of currently available drugs, treatment schedules, and long-term results. *Eur Urol*. 2008;53(1):45-52.
5. Babjuk M, Oosterlinck W, Sylvester R, Kaasinen E, Böhle A, Palou-Redorta J. EAU guidelines on non-muscle-invasive urothelial carcinoma of the bladder. *Eur Urol*. 2008;54(2):303-314.
6. Oeyen E, Hoekx L, De Wachter S, Baldewijns M, Ameye F, Mertens I. Bladder cancer diagnosis and follow-up: the current status and possible role of extracellular vesicles. *Int J Mol Sci*. 2019;20(4):821.
7. Tilki D, Singer BB, Shariat SF, et al. CEACAM1: a novel urinary marker for bladder cancer detection. *European Urol*. 2010;57(4):648-654.
8. Yu W, Hurley J, Roberts D, et al. Exosome-based liquid biopsies in cancer: opportunities and challenges. *Ann Oncol*. 2021;32(4):466-477.
9. Piccin A, Van Schilfgaarde M, Smith O. The importance of studying red blood cells microparticles. *Blood Transfus*. 2015;13(2):172-173.
10. Piccin A, Steurer M, Feistritzer C, et al. Observational retrospective study of vascular modulator changes during treatment in essential thrombocythemia. *Transl Res*. 2017;184:21-34.
11. Piccin A, Sartori MT, Bisogno G, et al. New insights into sinusoidal obstruction syndrome. *Intern Med J*. 2017;47:1173-1183.
12. Théry C, Witwer KW, Aikawa E, et al. Minimal information for studies of extracellular vesicles 2018 (MISEV2018): a position statement of the International Society for Extracellular Vesicles and update of the MISEV2014 guidelines. *J Extracell Vesicles*. 2018;7:3078.
13. Igami K, Uchiumi T, Ueda S, Kamioka K. Characterization and function of medium and large extracellular vesicles from plasma and urine by surface antigens and annexin V. *PeerJ Analytical Chem*. 2020;2:e4. doi:10.7717/peerj-achem.4
14. de Oliveira MC, Caires HR, Oliveira MJ, Fraga A, Vasconcelos MH, Ribeiro R. Urinary biomarkers in bladder cancer: where do we stand and potential role of extracellular vesicles. *Cancers (Basel)*. 2020;12(6):1-30.
15. Urabe F, Kimura T, Ito K, et al. Urinary extracellular vesicles: a rising star in bladder cancer management. *Transl Androl Urol*. 2021;10(4):1878-1889.
16. Ng K, Stenzl A, Sharma A, Vasdev N. Urinary biomarkers in bladder cancer: a review of the current landscape and future directions. *Urol Oncol Semin Orig Investig*. 2021;39(1):41-51.
17. Welton JL, Khanna S, Giles PJ, et al. Proteomics analysis of bladder cancer exosomes. *Mol Cell Proteomics*. 2010;9(6):1324-1338. doi:10.1074/mcp.M000063-MCP201
18. Serafini-cessi F, Malagolini N, Cavallone D. Tamm-Horsfall glycoprotein: biology and clinical relevance. *Am J Kidney Dis*. 2003;42(4):658-676. doi:10.1016/S0272-6386(03)00829-1
19. Carobolante G, Mantaj J, Ferrari E, Vllasaliu D. Cow milk and intestinal epithelial cell-derived extracellular vesicles as systems for enhancing oral drug delivery. *Pharmaceutics*. 2020;12(3):9-11.
20. Burillo J, Fernández-Rhodes M, Piquero M, et al. Human amylin aggregates release within exosomes as a protective mechanism in pancreatic β cells: pancreatic β-hippocampal cell communication. Biochim Biophys acta - Mol. *Cell Res*. 2021;1868(5):118971.
21. Sundar IK, Li D, Rahman I. Small RNA-sequence analysis of plasma-derived extracellular vesicle miRNAs in smokers and patients with chronic obstructive pulmonary disease as circulating biomarkers. *J Extracell Vesicles*. 2019;8(1). doi:10.1080/20013078.2019.1684816
22. Hatsugai M, Kato T. Proteomics in digestive diseases. *Seibutsu Butsuri Kagaku*. 2012;56(1):19-24.
23. Mabuchi R, Adachi M, Ishimaru A, Zhao H, Kikutani H, Tanimoto S. Changes in metabolic profiles of yellowtail (*Seriola quinqueradiata*) muscle during cold storage as a freshness evaluation tool based on GC-MS metabolomics. *Foods*. 2019;8(10):511.
24. Galindo-Prieto B, Eriksson L, Trygg J. Variable influence on projection (VIP) for orthogonal projections to latent structures (OPLS). *J Chemometr*. 2014;28(8):623-632.
25. Zhu G, Wang Y, Wang W, et al. Untargeted GC-MS-based metabolomics for early detection of colorectal cancer. *Front Oncologia*. 2021;11. doi:10.3389/fonc.2021.729512
26. Mateescu B, Kowal EJK, Van BBWM, Bartel S, Bhattacharyya SN. Obstacles and opportunities in the functional analysis of extracellular vesicle RNA – an ISEV position paper. *J Extracell Vesicles*. 2017;6. doi:10.3389/fonc.2021.729512
27. Jayachandran M, Miller VM, Heit JA, Owen WG. Methodology for isolation, identi fi cation and characterization of microvesicles in peripheral blood. *J Immunol Methods*. 2012;375(1–2):207-214. doi:10.1080/20013078.2017.1286095
28. Bachurski D, Schuldner M, Nguyen PH, et al. Extracellular vesicle measurements with nanoparticle tracking analysis–an accuracy and repeatability comparison between NanoSight NS300 and ZetaView. *J Extracell Vesicles*. 2019;8(1). doi:10.1080/20013078.2019.1596016

29. Chen I, Xue L, Hsu C, et al. Phosphoproteins in extracellular vesicles as candidate markers for breast cancer. *Proc Natl Acad Sci USA*. 2017;114(12):3175-3180.
30. Lombard-Banek C, Reddy S, Moody SA, Nemes P. Label-free quantification of proteins in single embryonic cells with neural fate in the cleavage-stage frog (*Xenopus laevis*) embryo using capillary electrophoresis electrospray ionization high-resolution mass spectrometry (CE-ESI-HRMS). *Mol Cell Proteomics*. 2016;15(8):2756-2768. doi:10.1074/mcp.M115.057760
31. Zhao L, Cong X, Zhai L, et al. Comparative evaluation of label-free quantification strategies. *J Proteomics*. 2020;215:103669. doi:10.1016/j.jprot.2020.103669
32. Lai Y, Ye J, Chen J, et al. UPK3A: a promising novel urinary marker for the detection of bladder cancer. *Urology*. 2010;76(2):514.e6-514.e11. doi:10.1016/j.urology.2009.11.045
33. Fu YP, Kohaar I, Rothman N, et al. Common genetic variants in the PSCA gene influence gene expression and bladder cancer risk. *Proc Natl Acad Sci USA*. 2012;109(13):4974-4979.
34. Wu WB, Jia GZ, Chen L, Liu HT, Xia SJ. Analysis of the expression and prognostic value of annexin family proteins in bladder cancer. *Front Genet*. 2021;12:1-13.
35. Hammarström S. The carcinoembryonic antigen (CEA) family: structures, suggested functions and expression in normal and malignant tissues. *Semin Cancer Biol*. 1999;9(2):67-81.
36. Kelleher M, Singh R, O'Driscoll CM, Melgar S. Carcinoembryonic antigen (CEACAM) family members and inflammatory bowel disease. *Cytokine Growth Factor Rev*. 2019;47:21-31. doi:10.1016/j.cytogfr.2019.05.008
37. Saeland E, Belo AI, Mongera S, Van Die I, Meijer GA, Van Kooyk Y. Differential glycosylation of MUC1 and CEACAM5 between normal mucosa and tumour tissue of colon cancer patients. *Int J Cancer*. 2012;131(1):117-128.
38. Chen J, Li Q, An Y, et al. CEACAM6 induces epithelial-mesenchymal transition and mediates invasion and metastasis in pancreatic cancer. *Int J Oncol*. 2013;43(3):877-885.
39. D'Souza-Schorey Crislyn C, Clancy JW. Tumor-derived microvesicles: shedding light on novel microenvironment modulators and prospective cancer biomarkers. *Genes Dev*. 2012;26(12):1287-1299.
40. Ma J, Zhang H, Tang K, Huang B. Tumor-derived microparticles in tumor immunology and immunotherapy. *Eur J Immunol*. 2020;50(11):1653-1662.
41. Xu P, Tang K, Ma J, et al. Chemotherapeutic tumor microparticles elicit a neutrophil response targeting malignant pleural effusions. *Cancer Immunol Res*. 2020;8(9):1193-1205.
42. Liu J, Ma J. Ke Tang and BH. Therapeutic use of tumor cell-derived extracellular vesicles. *Methods Mol Biol*. 2017;1660:433-440.
43. Mege D, Panicot-Dubois L, Dubois C. Tumor-derived microparticles to monitor colorectal cancer evolution. *Color Cancer Methods Protoc*. 2018;1765:271-277.
44. Yu M, Li T, Li B, et al. Phosphatidylserine-exposing blood cells, microparticles and neutrophil extracellular traps increase procoagulant activity in patients with pancreatic cancer. *Thromb Res*. 2020;188:5-16. doi:10.1016/j.thromres.2020.01.025
45. Zhao L, Bi Y, Kou J, Shi J, Piao D. Phosphatidylserine exposing-platelets and microparticles promote procoagulant activity in colon cancer patients. *J Exp Clin Cancer Res*. 2016;35(1):1-12. doi:10.1186/s13046-016-0328-9
46. Zhang C, Yang Z, Zhou P, et al. Phosphatidylserine-exposing tumor-derived microparticles exacerbate coagulation and cancer cell transendothelial migration in triple-negative breast cancer. *Theranostics*. 2021;11(13):6445-6460.
47. Crescitelli R, Lässer C, Szabó TG, et al. Distinct RNA profiles in subpopulations of extracellular vesicles: apoptotic bodies, microvesicles and exosomes. *J Extracell Vesicles*. 2013;2(1). doi:10.3402/jev.v2i0.20677
48. Van Deun J, Mestdagh P, Sormunen R, et al. The impact of disparate isolation methods for extracellular vesicles on downstream RNA profiling. *J Extracell Vesicles*. 2014;3(1). doi:10.3402/jev.v3.24858
49. Crescitelli R, Lässer C, Jang SC, et al. Subpopulations of extracellular vesicles from human metastatic melanoma tissue identified by quantitative proteomics after optimized isolation. *J Extracell Vesicles*. 2020;9(1):1722433.
50. Muturi HT, Dreesen JD, Nilewski E, et al. Tumor and endothelial cell-derived microvesicles carry distinct CEACAMs and influence T-cell behavior. *PLoS One*. 2013;8(9):e74654.
51. Zheng J, Hernandez JM, Doussot A, et al. Extracellular matrix proteins and carcinoembryonic antigen-related cell adhesion molecules characterize pancreatic duct fluid exosomes in patients with pancreatic cancer. *HPB*. 2018;20(7):597-604. doi:10.1016/j.hpb.2017.12.010
52. Yoshioka Y, Kosaka N, Konishi Y, et al. Ultra-sensitive liquid biopsy of circulating extracellular vesicles using ExoScreen. *Nat Commun*. 2014;5:3591.
53. Kabe Y, Suematsu M, Sakamoto S, et al. Development of a highly sensitive device for counting the number of disease-specific exosomes in human sera. *Clin Chem*. 2018;64(10):1463-1473.
54. Shao H, Im H, Castro CM, Breakefield X, Weissleder R, Lee H. New technologies for analysis of extracellular vesicles. *Chem Rev*. 2018;118(4):1917-1950.
55. Gandham S, Su X, Wood J, et al. Technologies and standardization in research on extracellular vesicles. *Trends Biotechnol*. 2020;38(10):1066-1098. doi:10.1016/j.tibtech.2020.05.012

SUPPORTING INFORMATION

Additional supporting information may be found in the online version of the article at the publisher's website.

How to cite this article: Igami K, Uchiumi T, Shiota M, et al. Extracellular vesicles expressing CEACAM proteins in the urine of bladder cancer patients. *Cancer Sci*. 2022;113:3120-3133. doi: 10.1111/cas.15438